Shape sensing using multi-core fiber optic cable and parametric curve solutions

Jason P. Moore* and Matthew D. Rogge

NASA Langley Research Center, Hampton, Virginia 23681, USA
**jason.p.moore@nasa.gov*

Abstract: The shape of a multi-core optical fiber is calculated by numerically solving a set of Frenet-Serret equations describing the path of the fiber in three dimensions. Included in the Frenet-Serret equations are curvature and bending direction functions derived from distributed fiber Bragg grating strain measurements in each core. The method offers advantages over prior art in that it determines complex three-dimensional fiber shape as a continuous parametric solution rather than an integrated series of discrete planar bends. Results and error analysis of the method using a tri-core optical fiber is presented. Maximum error expressed as a percentage of fiber length was found to be 7.2%.

OCIS codes: (060.3735) Fiber Bragg gratings; (060.2370) Fiber optics sensors; (120.6650) Surface measurements, figure; (120.3890) Medical optics instrumentation.

References and links

1. R. Kashyap, *Fiber Bragg Gratings,* 2nd ed. (Elsevier, 2010).
2. M. J. Gander, W. N. MacPherson, R. McBride, J. D. C. Jones, L. Zhang, I. Bennion, P. M. Blanchard, J. G. Burnett, and A. H. Greenaway, "Bend measurement using Bragg gratings in multi-core fiber," Electron. Lett. **36**(2), 120–121 (2000).
3. G. M. H. Flockhart, W. N. MacPherson, J. S. Barton, J. D. C. Jones, L. Zhang, and I. Bennion, "Two-axis bend measurement with Bragg gratings in multicore optical fiber," Opt. Lett. **28**(6), 387–389 (2003).
4. R. G. Duncan, M. E. Froggatt, S. T. Kreger, R. J. Seeley, D. K. Gifford, A. K. Sang, and M. S. Wolfe, "High-accuracy fiber-optic shape sensing," Proc. SPIE **6530**, 65301S, 65301S-11 (2007).
5. S. M. Klute, R. G. Duncan, R. S. Fielder, G. W. Butler, J. H. Mabe, A. K. Sang, R. J. Seeley, and M. T. Raum, "Fiber-optic shape sensing and distributed strain measurements on a morphing chevron," in *Proceedings of the 44th AIAA Aerospace Sciences Meeting and Exhibit* (Reno, Nevada, Jan. 9–12, 2006).
6. A. Gray, *Modern Differential Geometry of Curves and Surfaces* (CRC Press, 1993), Chap. 7.
7. J. Langer and D. A. Singer, "Lagrangian aspects of the Kirchhoff elastic rod," SIAM Rev. **38**(4), 605–618 (1996).
8. C. de Boor, *A Practical Guide to Splines* (Springer-Verlag, 2001), Chap. 14.
9. B. A. Childers, M. E. Froggatt, S. G. Allison, T. C. Moore, D. A. Hare, C. F. Batten, and D. C. Jegley, "Use of 3000 Bragg grating strain sensors distributed on four eight-meter optical fibers during static load tests of a composite structure," Proc. SPIE **4332**, 133–142 (2001).

1. Introduction

Fiber Bragg Grating (FBG) strain gauges have been and continue to be the subject of much investigation and reporting [1]. The use of the FBG strain gauge in the most typical form consists of inferring the strain at the surface of a material or structural member through the measurement of strain in a surface-bonded FBG. A less reported use of the FBG strain sensor is in providing strain information inside a multi-core optical fiber for the purpose of inferring bending in the fiber. Results of using axially co-located FBG sensors in multi-core fiber to make single-axis fiber bend measurements were first reported by Gander et al. [2] and the results of two-axis bending measurements using co-located FBG sensors were subsequently reported by Flockhart et al. [3]. While those results focused on local bending at a single FBG group at a single point along a fiber, the dense and distributed FBG interrogation ability of Optical Frequency Domain Reflectometer (OFDR) technology has led to an interest in using multi-core optical fiber for shape sensing [4]. Multi-core optical fiber containing low reflectivity, co-located FBG sensors provide a means of measuring distributed fiber curvature,

#159280 - $15.00 USD Received 2 Dec 2011; accepted 18 Jan 2012; published 24 Jan 2012

which can be processed to give an estimation of the shape and location of the fiber in three-dimensional space. A multi-core fiber optic shape and location sensor has potential applications in morphing-wing shape monitoring, minimally-invasive surgical catheter tracking, tethered-robot positional tracking, and undersea towed instrument tracking. Duncan et al. details a shape formulation method wherein a discrete set of curvature calculations derived from co-located FBG groups at discrete locations along the fiber are serially summed in the form of three-dimensional vector displacements to give fiber shape [4]. That method allows for error in its failure to account for the physical phenomenon of a natural twist that occurs in fiber as it is subjected to complex bending in three dimensions [5]. This paper reports a method of converting distributed curvature measurements into a three-dimensional shape by combining elastic rod theory and differential geometry to arrive at a three-dimensional solution of the Frenet-Serret formulas.

This paper is organized in the following manner. First, the Frenet-Serret formulas for three-dimensional curves and the relationship between the Frenet-Serret formulas and an optical fiber shape are explained. Secondly, the methods used to measure the discrete bending parameters of a tri-core optical fiber are outlined and the method of incorporating the bending parameters into a solution of the Frenet-Serret formulas is detailed. Results of using the methods to resolve the shape of a tri-core optical fiber as it is placed in a series of known curves in two and three dimensions are presented. A discussion of error sources and concluding remarks conclude the report.

2. Frenet-Serret formulas for curves in three dimensions

Curves in three-dimensional space can be described by a set of equations known as the Frenet-Serret formulas [6]. Let s represent the length along a curve in 3-D space and

$$\mathbf{r}(s) = x(s)\boldsymbol{i} + y(s)\boldsymbol{j} + z(s)\boldsymbol{k} \tag{1}$$

represent the location in R^3 of a point at length s along the curve. Then the Frenet-Serret *frame* can be defined by the tangent, normal, and binormal vectors. The tangent unit vector, $\mathbf{T}(s)$, defining the "pointing" direction of the curve is defined by

$$\mathbf{T}(s) = \frac{d\mathbf{r}(s)}{ds} = x'(s)\boldsymbol{i} + y'(s)\boldsymbol{j} + z'(s)\boldsymbol{k}, \tag{2}$$

where differentiation with respect to s is denoted by a prime ('). The normal unit vector, $\mathbf{N}(s)$, pointing in the direction of curvature, is defined by

$$\mathbf{N}(s) = \mathbf{T}'(s) = \frac{x''(s)\boldsymbol{i} + y''(s)\boldsymbol{j} + z''(s)\boldsymbol{k}}{\sqrt{(x''(s))^2 + (y''(s))^2 + (z''(s))^2}}, \tag{3}$$

The binormal unit vector, $\mathbf{B}(s)$, which points in the direction of zero curvature, and is orthogonal to both $\mathbf{N}(s)$ and $\mathbf{T}(s)$, is defined by

$$\mathbf{B}(s) = \mathbf{T}(s) \times \mathbf{N}(s). \tag{4}$$

The tangent, normal, and binormal unit vectors are related to each other according to the Frenet-Serret formulas:

$$\mathbf{T}'(s) = \kappa(s)\mathbf{N}(s); \mathbf{N}'(s) = -\kappa(s)\mathbf{T}(s) + \tau(s)\mathbf{B}(s); \mathbf{B}'(s) = -\tau(s)\mathbf{N}(s), \tag{5}$$

where $\kappa(s)$ and $\tau(s)$ are the scalar-valued curvature and torsion functions, respectively, of the curve. Curvature is defined as

$$\kappa(s) = \left\|\mathbf{T}'(s)\right\| = \sqrt{(x''(s))^2 + (y''(s))^2 + (z''(s))^2} \tag{6}$$

#159280 - $15.00 USD Received 2 Dec 2011; accepted 18 Jan 2012; published 24 Jan 2012

and can be qualitatively described as the rate at which the tangent unit vector changes in the direction of the normal unit vector. Torsion is defined as

$$\tau(s) = \frac{\left(\mathbf{r}'(s) \times \mathbf{r}''(s)\right) \cdot \mathbf{r}'''(s)}{\left\|\mathbf{r}'(s) \times \mathbf{r}''(s)\right\|^2} \tag{7}$$

and can be qualitatively described as the rate at which the normal unit vector changes in the direction of the binormal unit vector. If curvature and torsion are explicitly defined, the Frenet-Serret formulas can be solved and position can be determined using the Tangent unit vector through

$$\mathbf{r}(s) = \int \mathbf{T}(s) ds + \mathbf{r}_0, \tag{8}$$

where $\mathbf{r}_0$ is the initial location at $s = 0$.

3. Elastic tube theory and Frenet-Serret formulas

To relate the bending and twisting of the physical fiber to abstract three-dimensional curves described by Frenet-Serret formulas, we first assume that the fiber behaves as a uniform, symmetric, linear Kirchhoff rod, meaning it is of circular cross-section and uniform density [7]. Obviously, because of the cores and fiber coating, the assumptions of uniform density and symmetry are immediately violated; however, the violations of the assumptions become significant only during tight bending configurations. The Kirchhoff rod assumption leads to an easily defined relationship between the material fiber frame and the natural curve frame along which it lies. If the fiber is free-sleeved, meaning it resides inside of a frictionless (ideal) constraint, and is fully secured only at one end, the relationship between the material fiber frame and the natural curve frame will remain constant along the fiber. Langer and Singer [7], pp. 607-609, provides an in-depth discussion of this theory. In the case of multi-core fiber shape sensing, free-sleeving the fiber enables manipulation of the fiber into complex curves without inducing external twisting forces into the fiber. This configuration also asserts that the angular orientation of the cores at fiber length zero holds throughout the length of the fiber and that all derived torsion (shown previously in Eq. (7) and addressed later in Eq. (15)) is a consequence of the arbitrary curve or shape the fiber follows.

4. Bending measurements in three dimensions along the fiber

In order to deduce the bending direction and radius of curvature in three dimensions, at least three separate core strains must be measured, and it is the case of symmetrically arranged tri-core fiber on which this paper focuses. Figure 1 details the cross-sectional layout of a typical symmetric tri-core fiber.

#159280 - $15.00 USD Received 2 Dec 2011; accepted 18 Jan 2012; published 24 Jan 2012

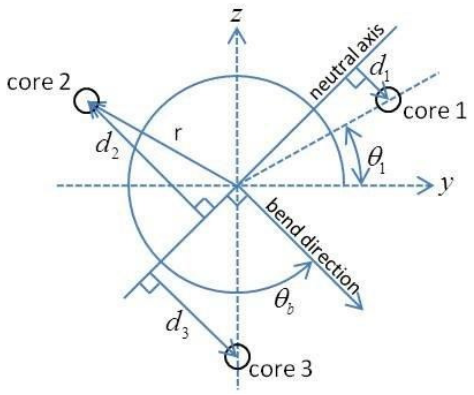

Fig. 1. Typical symmetrical tri-core geometry and parameters for determining strain due to bending.

The locations of the cores in the cross section of the fiber are defined by a radial offset from the center, r, and an angular separation of $2\pi/3$ with θ_1 representing the offset of core 1 from the $\theta = 0$ axis. Not shown in Fig. 1 are the cladding boundary and fiber coating. The orientation of the cores relative to the material frame of the fiber is set by θ_1 and, as explained prior, is assumed to be constant throughout the fiber. The value of θ_1 is typically set using the simple calibration method of bending the fiber in a known single plane, measuring the strain values in the cores, and determining the value based on the measured strain values and knowledge of the bending plane.

Figure 1 also shows the geometrical relationships of the three cores in an arbitrary bending configuration. The relationship between core-specific FBG strain values and the curvature of the fiber at the axial location of the FBG's has been shown to be

$$\Delta\varepsilon = \varepsilon_2 - \varepsilon_1 = \frac{d}{R} = \frac{d_1 + d_2}{R}, \tag{9}$$

where ε_1 and ε_2 are the strain values of core 1 and 2 FBG's, respectively, R is the bend radius of the fiber, and d is the distance between the two cores respective to the bending plane of the fiber [2]. Modifying Eq. (9) in order to express strain dependence as a function of core distance from the neutral bend axis (zero strain) and using the inverse relationship of curvature and radius of curvature (κ = 1/R) gives a general expression for strain in a given core due to bending:

$$\varepsilon_i = -\kappa r_i \cos\left(\theta_b - 3\pi/2 - \theta_i\right), \tag{10}$$

where ε_i is the axial strain at the i^{th} core, r_i is distance from the i^{th} core to center of fiber, θ_b is the angular offset from the local y-axis to the fiber bending direction, and θ_i is the angular offset from the local y-axis to the core. Though this paper deals with the results of a symmetric tri-core fiber, Eq. (10) applies to any number of cores in any arrangement, symmetrical or asymmetrical. Previous works calculate curvature by comparing strain measurements in pairs of cores. While this method is mathematically sufficient, strain measurement error can lead to large curvature errors. To calculate curvature using information from all cores and reduce the sensitivity to error in a single strain measurement, we first define an apparent curvature vector which points in the direction of the i^{th} core from the center of the fiber:

$$\boldsymbol{\kappa}_{app,i} = -\frac{\varepsilon_i}{r_i}\left(\cos\theta_i \mathbf{j} + \sin\theta_i \mathbf{k}\right), \tag{11}$$

#159280 - $15.00 USD Received 2 Dec 2011; accepted 18 Jan 2012; published 24 Jan 2012

where unit vectors $\boldsymbol{j}$ and $\boldsymbol{k}$ align with the local y- and z-axes, respectively. Note that the magnitude of each core's apparent local curvature vector is dependent on its measured strain and radial distance from the center of the fiber while the vector direction depends on the angular offset of the core. For N number of cores in the fiber, the vector sum of the apparent curvature vectors is formulated as

$$\boldsymbol{\kappa}_{app} = -\sum_{i=1}^{N} \frac{\varepsilon_i}{r_i} \cos\theta_i \boldsymbol{j} - \sum_{i=1}^{N} \frac{\varepsilon_i}{r_i} \sin\theta_i \boldsymbol{k}. \tag{12}$$

For the symmetric case in which each core is distance r from the center of the fiber, substituting Eq. (10) for the strain and applying trigonometric identities gives

$$\kappa = \frac{2\left|\boldsymbol{\kappa}_{app}\right|}{N} = \frac{2\sqrt{\left(\sum_{i=1}^{N} \varepsilon_i \cos\theta_i\right)^2 + \left(\sum_{i=1}^{N} \varepsilon_i \sin\theta_i\right)^2}}{Nr}. \tag{13}$$

Local bend direction is then

$$\theta = angle\left(\boldsymbol{\kappa}_{app}\right). \tag{14}$$

The calculations of Eqs. (13) and (14) are repeated for every FBG triplet along the fiber to create discrete sets of curvature ($\kappa_{n\,=\,0\ldots N}$) and bend direction ($\theta_{n\,=\,0\ldots N}$) at specific locations ($s_{n\,=\,0\ldots N}$) along the fiber corresponding to co-located FBG groups.

5. Solving for shape

The discrete measurements of curvature and bend direction are fitted using a cubic smoothing spline with smoothing parameter equal to 0.99 for the curvature function and 0.95 for the bend direction [8] to give explicit functions of curvature $\kappa(s)$ and bend direction $\theta(s)$ vs. fiber length. The bend direction function is then differentiated with respect to length to give an explicit torsion function:

$$\tau(s) = \theta'(s). \tag{15}$$

The Frenet-Serret formulas of Eq. (5) and the corresponding fiber position relationship of Eq. (8) can be solved numerically after explicit functions of curvature and torsion are found. Because the multi-core fiber is typically secured at a known location in a zero-curvature configuration at $s_0 = 0$, $\kappa_0 = \theta_0 = 0$ is specified prior to curve fitting the curvature and bend direction measurements, and initial conditions of the Frenet-Serret frame and fiber position are specified at $s_0 = 0$. The initial condition for position at fiber length zero is dictated by the actual physical position of the fiber in the global reference frame. The trivial choice is

$$\mathbf{r}_0 = (x_0, y_0, z_0) = (0,0,0). \tag{16}$$

The tangent vector initial value, $\mathbf{T}_0$, is also dictated by the actual physical position of the fiber at (x_0,y_0,z_0), in that $\mathbf{T}_0$ must be "pointing" in the direction of increasing fiber length at $s_0 = 0$ in the global reference frame. A trivial choice is along a single axis; such is the case for the data presented in this paper, where $\mathbf{T}_0$ is set equal to unit vector $\boldsymbol{i}$. The normal vector initial value, $\mathbf{N}_0$, is determined from the curve-fitted value of $\theta(0)$ The specification of $\mathbf{N}_0$ is made in the global reference frame and acts to relate the fiber local reference frame to global reference frame at $s_0 = 0$. For the data presented in this paper, $\mathbf{T}_0$ points along the x-axis so $\mathbf{N}_0$ must be located somewhere in the y-z plane. Arbitrarily chosen, $\theta = 0$ points along the y-axis and $\theta = \pi/2$ points along the z-axis. Therefore $\mathbf{N}_0$ is found by

$$\mathbf{N}_0 = \cos\left(\theta(0)\right)\boldsymbol{j} + \sin\left(\theta(0)\right)\boldsymbol{k}. \tag{17}$$

The binormal vector initial value, $\mathbf{B}_0$, is found using the Frenet-Serret frame relationship of Eq. (4) and substituting the initial tangent and normal vectors. With initial conditions

#159280 - $15.00 USD Received 2 Dec 2011; accepted 18 Jan 2012; published 24 Jan 2012

specified, Eqs. (5) and (8) can be solved using numerical methods to give location of the fiber vs. fiber length as well as the tangent, normal and binormal vectors along the fiber.

6. Experimental measurements

A symmetrical tri-core fiber with 68 µm radial core distance, 330 µm cladding diameter, and 510 µm coated diameter was placed in templates with eight shapes in total. The templates were made by CNC machining grooves in high-density polyethylene plates and cylinders. In order to reduce friction between the fiber and the template, the fiber was fed through a 20 gauge fiberglass sleeve that was then placed in the grooves in the templates and held in place by Kapton® tape. The fiber has fiber Bragg gratings co-located in each core at 10 mm intervals along the fiber. The grating wavelengths were measured using a three-channel Optical Frequency Domain Reflectometer (OFDR) [9] system and baseline grating wavelengths were determined while the fiber was secured in a straight line. The wavelength data was converted to strain data using a strain per wavelength change relationship of 860.2 $\mu\varepsilon$ /Δnm and strain data was processed to shape solutions as described previously. Measured shape error is calculated by subtracting the known coordinates of the curve from the measured shape.

The first template is a plate with five grooves machined into its surface. The grooves, denoted P1 through P5, follow planar curves of 84 cm total arc-length with maximum curvatures ranging from 10 to 70 m^{-1}. The grooves are located on the surface such that the fiber experiences a region of zero curvature followed by a single bend and then another region of zero curvature. The second template is made from a 0.12 m radius, 0.6 m long cylinder and has three grooves, denoted C1, C2, and C3, machined into its surface. The arc-lengths of curves C1, C2, and C3 are 1.03, 1.11, and 1.68 m, respectively. The grooves are defined by parametric curves in cylindrical coordinates with constant radius. The Y-X and Z-θ relationships for the two- and three-dimensional reference curves are shown in Figs. 2(a) and 2(b) along with a three-dimensional representation of shape C1 in Fig. 2(c).

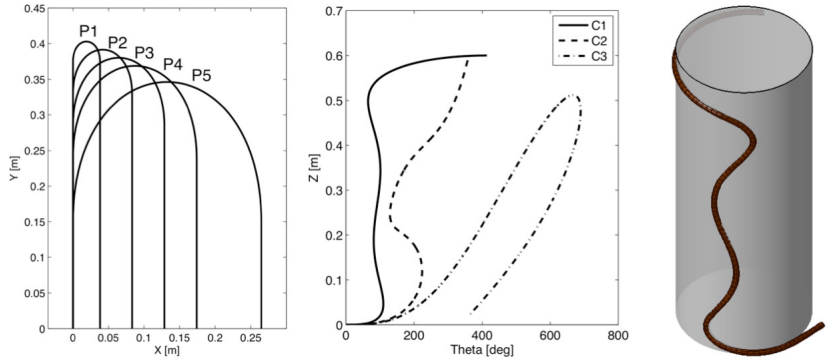

(a) (b) (c)

Fig. 2. (a) Y vs. X for curves P1 - P5. (b) Z vs. θ of curves C1-C3.

7. Results

The absolute measured shape error and error per unit length at each grating triplet for planar curves P1-5 is shown in Fig. 3. Maximum error per unit length in the planar configurations is 1.68%, occurring in curve P3 with 8.07 mm error at 0.48 m along the fiber. The primary components of the errors in shapes P1-P5 are deviations from the curve plane and are most likely caused by the fiberglass sleeve applying twisting loads to the fiber as it deforms under tight bends.

#159280 - $15.00 USD Received 2 Dec 2011; accepted 18 Jan 2012; published 24 Jan 2012

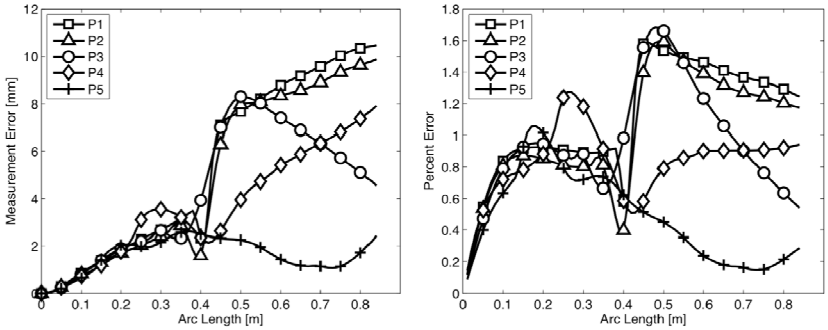

(a) (b)

Fig. 3. (a) Absolute measurement error and (b) error per unit length versus arc length for planar curves P1-P5.

The absolute measured shape error and error per unit length at each grating triplet the three-dimensional curves C1-C3 are shown in Fig. 4. Maximum error per unit length in the three-dimensional configurations is 7.22%, occurring in curve C2 with 31.06 mm error at 0.43 m along the fiber. Similar to the planar cases, the error is most likely due to the fiberglass sleeve applying twisting loads to the fiber. Root mean square, maximum absolute, maximum percentage and end errors for each shape are presented in Table 1.

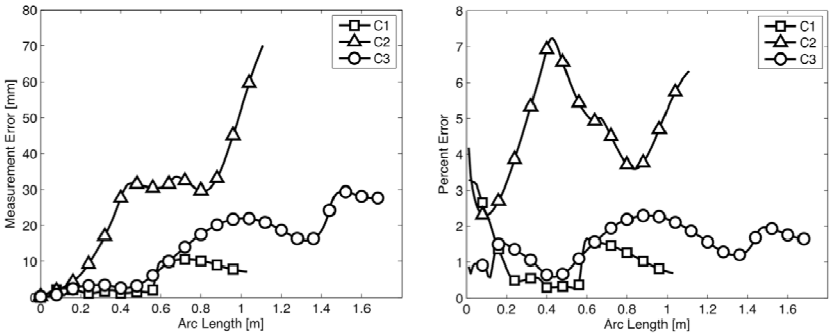

(a) (b)

Fig. 4. (a) Absolute measurement error and (b) error per unit length versus arc length for three-dimensional curves C1-C3.

Table 1. Measurement Error Statistics

	P1	P2	P3	P4	P5	C1	C2	C3
Fiber Length [m]	0.84	0.84	0.84	0.84	0.84	1.03	1.11	1.68
RMSE [mm]	4.77	6.25	6.72	5.87	3.68	6.34	32.58	16.93
Max. Error [mm]	9.51	10.95	10.80	9.27	5.76	10.53	70.07	29.46
Max. % Error [%]	1.59	1.60	1.68	1.27	1.06	3.28	7.22	2.30
End Error [mm]	5.80	5.22	6.62	5.98	3.65	7.15	70.07	27.66

8. Conclusion

A new method of calculating the shape of a multi-core fiber optic cable has been presented. The method utilizes discrete strain measurements obtained in each core to create a continuous representation of fiber curvature and torsion. The Frenet-Serret equations are then solved using these representations to obtain fiber shape. Shape measurements were found to have at most 7.2% error. The primary source of error is most likely externally induced twisting in the fiber. Future work will focus on elimination of this error by incorporating twist measurements into the shape solution.

#159280 - $15.00 USD Received 2 Dec 2011; accepted 18 Jan 2012; published 24 Jan 2012